The EMBO Journal vol.14 no.5 pp.1015–1023, 1995

Crystal structure of casein kinase-1, a phosphate-directed protein kinase

Rui-Ming Xu, Gilles Carmel[1], Robert M.Sweet[2], Jeff Kuret[1,3] and Xiaodong Cheng[3]

W.M.Keck Structural Biology Laboratory, Cold Spring Harbor Laboratory, Cold Spring Harbor, NY 11724, [1]MGC Corp., 101 Waukegan Road, Lake Bluff, IL 60044 and [2]Biology Department, Brookhaven National Laboratory, Upton, NY 11973, USA

[3]Corresponding authors

Communicated by J.D.Watson

The structure of a truncated variant of casein kinase-1 from *Schizosaccharomyces pombe*, has been determined in complex with MgATP at 2.0 Å resolution. The model resembles the 'closed', ATP-bound conformations of the cyclin-dependent kinase 2 and the cAMP-dependent protein kinase, with clear differences in the structure of surface loops that impart unique features to casein kinase-1. The structure is of unphosphorylated, active conformation of casein kinase-1 and the peptide-binding site is fully accessible to substrate.

Key words: casein kinase-1/nucleotide binding/protein kinase regulation/substrate specificity/structural similarity

Introduction

Casein kinase-1 (CK1) is a family of protein kinases common to all eukaryotic cells (Tuazon and Traugh, 1991; Issinger, 1993). These enzymes phosphorylate many proteins *in vitro*, including SV40 T-antigen (Cegielska and Virshup, 1993), glycogen synthase (Kuret *et al.*, 1985; Roach, 1991), the transcriptional regulators CREM (De Groot *et al.*, 1993) and p53 (Milne *et al.*, 1992). CK1 phosphorylation alters the activity of each of these substrates, and is necessary for full origin unwinding activity of T-antigen. In lower eukaryotes, individual CK1 isoforms perform essential functions in both the cytoplasm and nucleus, where they participate in the regulation of DNA repair pathways and cell morphogenesis (Hoekstra *et al.*, 1991; Robinson *et al.*, 1992; Wang *et al.*, 1992). In addition to its roles in normal cells, CK1 has been implicated in the pathogenesis of Alzheimer's disease through the hyperphosphorylation of tau protein, the major component of neurofibrillary tangles (Vincent and Davies, 1993).

To carry out its biological function, CK1 employs a catalytic domain that differs from most other protein kinases. Initially, on the basis of sequence alignments (Wang *et al.*, 1992), it contains neither the peptide triplet Ala-Pro-Glu in subdomain VIII nor the Arg residue in subdomain XI (Hanks *et al.*, 1988). In other protein kinases, these subdomains interact to form a Glu−Arg ion pair (Knighton *et al.*, 1991a; De Bondt *et al.*, 1993). Secondly, CK1 isoforms invariably retain high contents of lysines and arginines, resulting in unusually high isoelectric points (pI >9). Thirdly, the substrate selectivity of CK1 appears to be directed toward phosphate groups rather than unmodified amino acids. Evidence for this selectivity comes from studies with synthetic peptide substrates derived from CK1-specific phosphorylation sites in β-casein (Ser22: Meggio *et al.*, 1991), glycogen synthase (Ser10: Flotow *et al.*, 1990; Flotow and Roach, 1991) and SV40 T-antigen (Ser123: Umphress *et al.*, 1992). Results from all three systems point to the presence of acidic residues N-terminal to a phosphorylatable hydroxyamino acid as the minimal requirement for recognition of synthetic peptides by CK1. For example, the peptide DDDEESITRR is a substrate for CK1 (the underlined serine is the phosphate acceptor), but is phosphorylated with a K_M value in the millimolar range (Meggio *et al.*, 1991). Replacement of the aspartates with phosphoserines, however, results in substrates that are phosphorylated with higher k_{cat}/K_M values (Meggio *et al.*, 1991; Wang *et al.*, 1993). Phosphoserine has the greatest impact on substrate selectivity when placed at position P^{-3} (i.e. three residues N-terminal to the phosphorylatable hydroxyamino acid). Thus, CK1 isoforms appear to selectively recognize the sequence -S(P)XXS-, where X is any amino acid.

To learn more about the unusual structural features of CK1, we crystallized a C-terminal deletion mutant of Cki1 (Carmel *et al.*, 1994), one of four CK1 isoforms in fission yeast (Wang *et al.*, 1994). The truncation, termed Cki1Δ298, eliminates the C-terminal 148 amino acids of Cki1. Although the role of C-terminal domain is not fully understood, part of its function is to target the enzyme to membranes (Wang *et al.*, 1994). The 298-residue catalytic core of Cki1 is active catalytically (Carmel *et al.*, 1994), is nearly identical in length to cyclin-dependent kinase 2 (Cdk2) and corresponds to residues 37–319 of cAMP-dependent protein kinase (cAPK). Here we report the crystal structure of Cki1Δ298 in complex with MgATP at 2.0 Å resolution, and compare it with the structures of other protein kinases: the 2.2 Å-resolution model of the ternary complex of mammalian cAPK (pdb code 1ATP; Zheng *et al.*, 1993) and the 2.4 Å-resolution model of the binary complex of human Cdk2 (De Bondt *et al.*, 1993). The resultant CK1 model suggests how the substrate selectivity of this enzyme family is achieved.

Results

Quality of the model

Refinement statistics for Cki1Δ298 crystallized in a trigonal lattice are summarized in Table I. The current model consists of 288 of 298 possible residues, one complete molecule of ATP, one Mg^{2+} ion, and 103 water molecules.

Table I. Crystallographic data and refinement

Data collection			
Space group	$P3_221$		
Unit cell (Å)	$a = b = 78.96$	$c = 120.38$	
	Native	*p*CMBS	Dimercurial
Number of crystals	8	2	8
Total measurements	161782	76281	66555
Unique reflections	24245	16824	15755
R_{merge}[a] (%)			
isomorphous	8.04	7.93	8.66
anomalous	2.35	5.50	5.44
Resolution range (Å)	Completeness (%)		
20.0–2.71	93.9	92.0	92.2
11.3–3.95	94.3		
3.95–3.16	97.2		
3.16–2.76	93.4		
2.76–2.52	88.4		
2.52–2.34	82.8		
2.34–2.20	74.6		
2.20–2.09	65.1		
2.09–2.00	44.2		
Phasing			
Hg sites (number)	–	2	2
Phasing power[b] at 3 Å			
Isomorphous	–	1.08	1.37
Anomalous	–	2.02	2.03
Figure of merit at 3 Å	0.684		
Refinement			
Resolution range (Å)	Reflections (number)	*R*-factor[c] (%)	
11.3–2.00	23860	20.7	
6.0–2.00	22976	19.5	
Protein atoms	2386		
ATP atoms	32		
Ordered water molecules	103		
Sulfate atoms	10		
R.m.s. deviation from ideality			
Bond lengths	0.008 Å		
Bond angles	1.46°		

[a] R_{merge} of isomorphous data = $\Sigma|I-\langle I\rangle|/\Sigma\langle I\rangle \times 100$, where I is the measured intensity of each reflection, and $\langle I\rangle$ is the intensity averaged from multiple observations of symmetry related reflections. R_{merge} of anomalous data = $\Sigma|\langle I+\rangle-\langle I-\rangle|/\Sigma(\langle I+\rangle+\langle I-\rangle) \times 100$, where $I+$ and $I-$ are the measured intensities of each Bijvoet pair.
[b] Phasing power = r.m.s.$(\langle F_H\rangle/E)$, where F_H is the heavy atom structure factor amplitude and E is the residual lack of closure.
[c] R-factor = $\Sigma|F_o-F_c|/\Sigma|F_o|$, where F_o and F_c are the observed and calculated structure factor amplitudes, respectively.

It also contains two sulfate ion-binding sites which are described in detail below. The model has been refined to an *R*-factor of 20.7% using all measured data (Table I). Two disordered chain segments could not be modelled: four residues (Ser2–Asn5) from the N-terminus (the initiating formyl-methionine was removed by cotranslational processing during expression; Carmel *et al.*, 1994) and five residues spanning Lys222–Asn226.

All main chain dihedral angles fall within allowed regions of the Ramachandran plot (Ramachandran *et al.*, 1963) except those for Val10, which was modeled with unfavorable angles ($\Phi = 67°$, $\Psi = -44°$). This assignment appears correct because the electron density surrounding Val10 clearly indicates the position of the carbonyl oxygen in addition to its side chain. We suspect that crystal packing constraints force Val10, which is preceded by a glycine and lies in a sharp turn just N-terminal to strand β1, into an unfavorable conformation.

Overall structure

The backbone structure of CK1 is shown in Figure 1. The structure contains nine α helices and nine β strands, designated A–I for helices and 1–9 for strands from N- to C-terminus of the sequence. The loops are designated by their flanking secondary structures. The protein folds into a small N-terminal lobe (amino acids 6–86) and a large C-terminal lobe (amino acids 92–298), connected by a single loop (L-5B; amino acids 87–91). The cleft lying between the two lobes binds nucleotide substrate.

The small N-terminal lobe contains five twisted antiparallel strands (β1–β5), one helix (αA), and the glycine-rich sequence motif, Gly19-Glu-Gly-Ser-Phe-Gly-Val25. As in other kinases, this motif forms a β1–turn–β2 structure over the nucleotide-binding site. Because β strands predominate in the N-terminal lobe, we term it the beta lobe. In contrast, the C-terminal lobe contains four long helices (αC, αE, αH, and αI) in an antiparallel

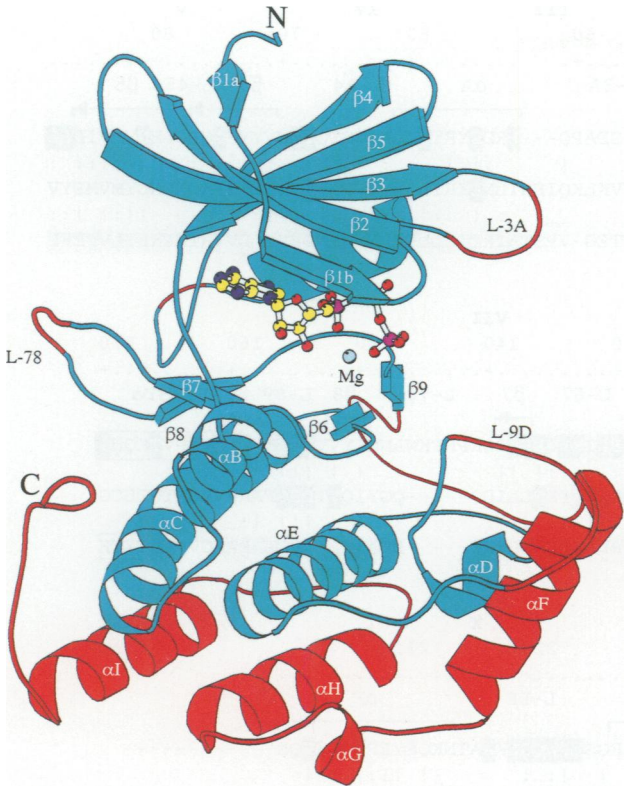

Fig. 1. The ribbon diagram of the molecular structure of CK1. The Cki1 catalytic domain folds into two lobes, one dominated by strands (β lobe), the other by helices (α lobe). MgATP in ball-and-stick is bound in the cleft between them. The most similar regions (with r.m.s. deviation <2.5 Å) among cAPK, Cdk2, and CK1 are shown in blue, whereas the less similar regions are shown in red. Although residues Lys222−Asn226 are disordered in the model, a main chain between Leu221 and Lys227 (the red part of loop L-EF) is connected to aid tracing of the polypeptide chain.

bundle with a fifth long helix (αF) almost perpendicular to the bundle. Together these helices establish the structural scaffold for the lobe, which we term the alpha lobe. The remainder of alpha lobe contains three short helices (αB, αD and αG), four short strands (β6−β9), and the long loops L-9D, L-EF and L-HI. Although strands β6 and β9 span only two residues, their main chain atoms form two β-strand-like hydrogen bonds. These short secondary structures and loops are clustered around the surface of the cleft and may be crucial for the function of the enzyme.

Comparison with other kinases

The conformation of nucleotide-bound CK1 resembles the 'closed', ligand-bound conformations of both cAPK (Zheng *et al.*, 1993) and Cdk2 (De Bondt *et al.*, 1993). Overall, many of the secondary structural elements are arranged similarly in the three enzymes. Disregarding any deletions and insertions among these enzymes in loop regions such as L-3A, L-78 and L-9D, the 179 Cα atoms in CK1 can be superimposed with cAPK within a root-mean-square (r.m.s.) difference of 1.8 Å. This region covers strands β1−β9, and helices αA−αE (Figures 1 and 2). The same set of Cα atoms results in r.m.s. differences of 2.5 Å between CK1 and Cdk2 and 2.1 Å between cAPK and Cdk2. Outside this core region, three helices of CK1 differ in orientations (αF and αH) and in length (αI) relative to those in cAPK and Cdk2.

Greater conformational differences appear in surface loops. Initially, in the beta lobe, the tip of the glycine-rich loop (L-12) lies in different conformations in each kinase, with CK1 tilted away from the cleft, Cdk2 tilted toward the cleft, and cAPK in between. The distance between Cα of Phe23 in CK1 and Phe54 in cAPK is 2.2 Å, whereas the distance between Phe23 in CK1 and Tyr15 in Cdk2 is 3.9 Å. The tilt toward the substrate-binding site observed for cAPK and Cdk2 relative to CK1 may be induced by the peptide inhibitor of cAPK, and the interaction with the inhibitory T-loop in Cdk2. Secondly, L-3A in CK1 replaces helix αB in cAPK, and a dissimilar loop in Cdk2. Thirdly, the loops equivalent to L-78, L-9D and L-HI vary greatly in both size and conformation among the three kinases.

Nucleotide-binding site

ATP binds to a cleft located between the alpha and beta lobes (see Figures 1, 3 and 4). Although the adenine and ribose rings are ordered in the structure, the β- and γ-phosphates appear somewhat flexible as indicated by their higher thermal factors. This may result from partial hydrolysis of the ATP during cocrystallization, or due to dynamic movement in the binary complex. ATP interacts with CK1 through both direct and water-mediated contacts. Its adenine base and ribose ring insert into a hydrophobic pocket formed by three Leu (amino acids 87, 88 and 138), three Ile (amino acids 18, 26 and 85), two Val (amino acids 38 and 153), and one Ala (amino acid 39).

In addition to the hydrophobic interactions, the N1 and N6 atoms of the adenine base hydrogen bond to the main chain nitrogen of Asp86 and Leu88 respectively, whereas N7 participates in a hydrogen bond cascade formed by two water molecules and the side chains of Glu55 and Tyr59. These interactions differ from those observed in cAPK, where N7 contacts Thr183 directly (Bossemeyer *et al.*, 1993; Zheng *et al.*, 1993), and in Cdk2, where only one hydrogen bond through N6 is observed (De Bondt *et al.*, 1993). Thus, one can appreciate how inhibitors that compete with nucleotide substrate, such as the CK1-selective isoquinoline sulfonamide CKI7 (Chijwa *et al.*, 1989), achieve their specificity.

The ribose ring adopts a 3′-endo-2′-exo twist with major 3′ and minor 2′ puckering and an anti-clinal glycosidic angle $\chi = -143°$. This conformation resembles that observed in the active ternary complex of cAPK, but differs from the inactive binary complex of Cdk2 (with 3′-exo-2′-endo, 3′ minor and 2′ major and $\chi = -118°$). The O3′ atom of ribose forms one direct hydrogen bond with the main chain carbonyl of Asp135. In contrast, the O2′ atom interacts with the side chains of Ser91 and Asp94 via two water molecules. The decapeptide segment (Asp86−Leu95) involved in the interactions with both adenine base and ribose ring is conserved throughout the CK1 family. This sequence bridges the two lobes and spans the presumptive hinge region (Karlsson *et al.*, 1993).

The triphosphate moiety of ATP interacts with three charged residues, Lys41, Lys133 and Asp154, and with Ser22 and the backbone amide of Gly24 in the glycine-rich loop (L-12). Nearly identical interactions exist in cAPK. However, the β-phosphate and side chains of homologs of Lys41 and Asp154 adopt different conformations in Cdk2 (De Bondt *et al.*, 1993). Four of five

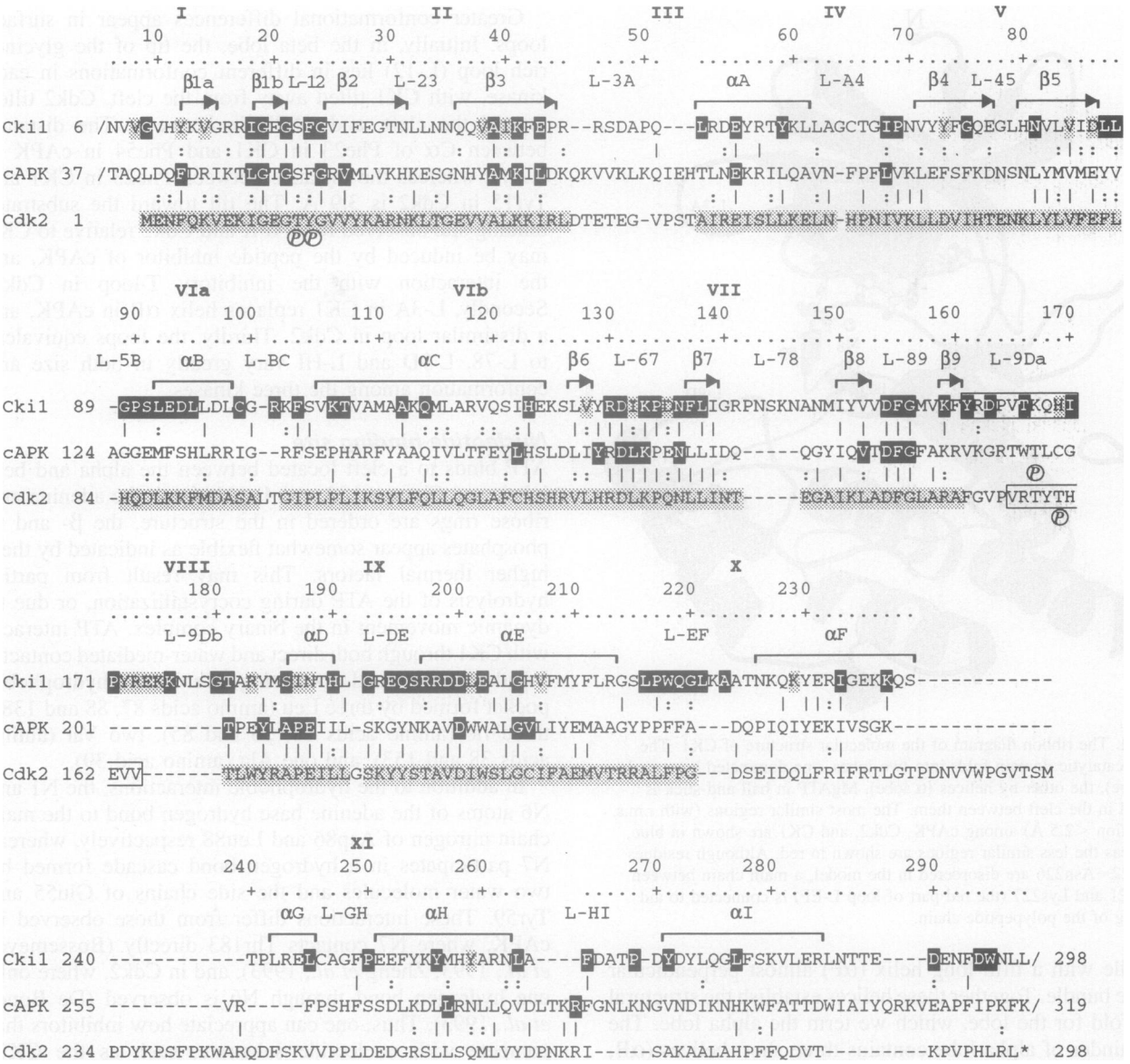

Fig. 2. Structure-based amino acid sequence alignment of yeast Cki1$^{6-298}$, human Cdk2, and mouse cAPK$^{37-319}$. Identities between pairs of kinases are shown with vertical bars, whereas similarities, grouped as (V, L, I, M), (F, Y, W), (K, R), (E, D), (Q, N), (S, T) and (A, G, P), are indicated by colons. Of CK1 and cAPK, 50 (17%) amino acids are identical and 42 (14%) are similar. Roman numerals mark the beginning of each of the eleven protein kinase subdomains identified by Hanks *et al.* (1988). Numbering and secondary structure elements are shown for Cki1$^{6-298}$. Phosphorylation sites are indicated by the circled letter P. Residues highlighted in Cki1$^{6-298}$ are either invariant (white against black) or similar (shaded) in all known isoforms of CK1 (Kearney *et al.*, 1994). Residues highlighted in cAPK are those identified as being conserved in most protein kinases. Residues highlighted in Cdk2 correspond to the core region with r.m.s. deviation <2.5 Å among the three structures.

invariant residues, Lys41 in β3, Glu55 in αA, Asp131 in L-67, Asp154 in L-89 and Asp200 in αE, found in protein kinases (Hanks *et al.*, 1988) interact directly (Lys41 and Lys133) or indirectly (Glu55 and Asp131) with the triphosphate moiety. Like other protein kinases, CK1 retains the catalytic loop Asp131-Ile-Lys-Pro-Asp-Asn136 (L-67), suggesting that the catalytic mechanism of CK1 will resemble that of cAPK (Knighton *et al.*, 1991a; Bossemeyer *et al.*, 1993) and other characterized protein kinases.

One Mg^{2+} is found in CK1, where it bridges the α- and γ-phosphates (Figure 3), and lies in a position corresponding to the low-affinity metal-binding site of cAPK. When the two proteins are superimposed, the two ions are 1.2 Å apart. The Mg^{2+} in CK1 is coordinated by Asn136 alone, a residue common to all Ser/Thr kinases, while the side chain of Asp154 is 3.7 Å away. Two residues (the homologs of Asn136 and Asp154) coordinate this site in both cAPK and Cdk2.

Structural basis of substrate selectivity

On the basis of kinetic measurements, CK1 selectively binds synthetic peptide substrates containing a phospho-amino acid at position P^{-3}. This requirement differs dramatically from that of cAPK, which selectively binds positively charged residues in positions P^{-2} and P^{-3}. Not surprisingly, the key residues involved in substrate binding in cAPK, Glu127, Glu170 and Glu230, have no analogs in CK1. The main chain positions of these three glutamic acids are replaced by Ser91, Asp135 and Tyr210

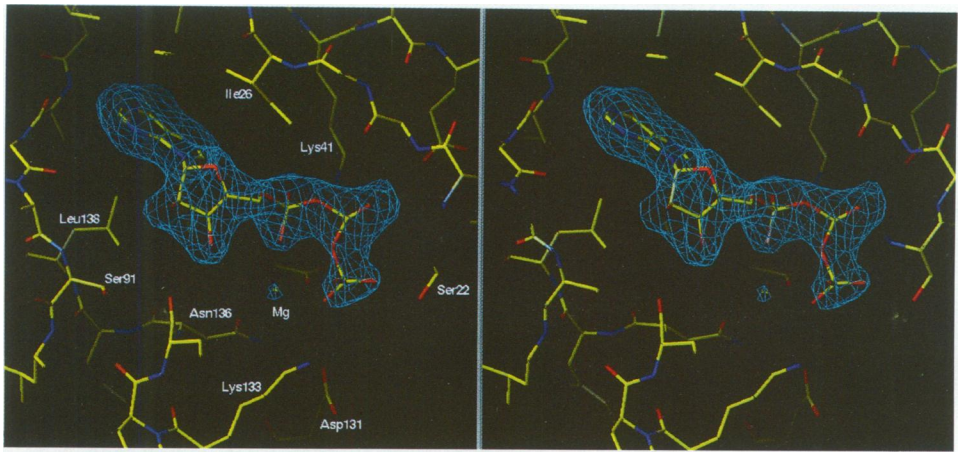

Fig. 3. The structure of MgATP in binary complex with CK1. Stereo view of a difference electron density map (F_o-F_c, α_c) contoured at 3σ above the mean. The MgATP was omitted in the structure factor calculation. Mg^{2+} makes direct contact with the α- and γ-phosphates, and $O_{\delta 1}$ of Asn136. This position corresponds to the low-affinity M1 site of cAPK (Bossemeyer *et al.*, 1993; Zheng *et al.*, 1993). No density is apparent for a homolog of the high-affinity Mg^{2+}-binding site (M2) found in cAPK.

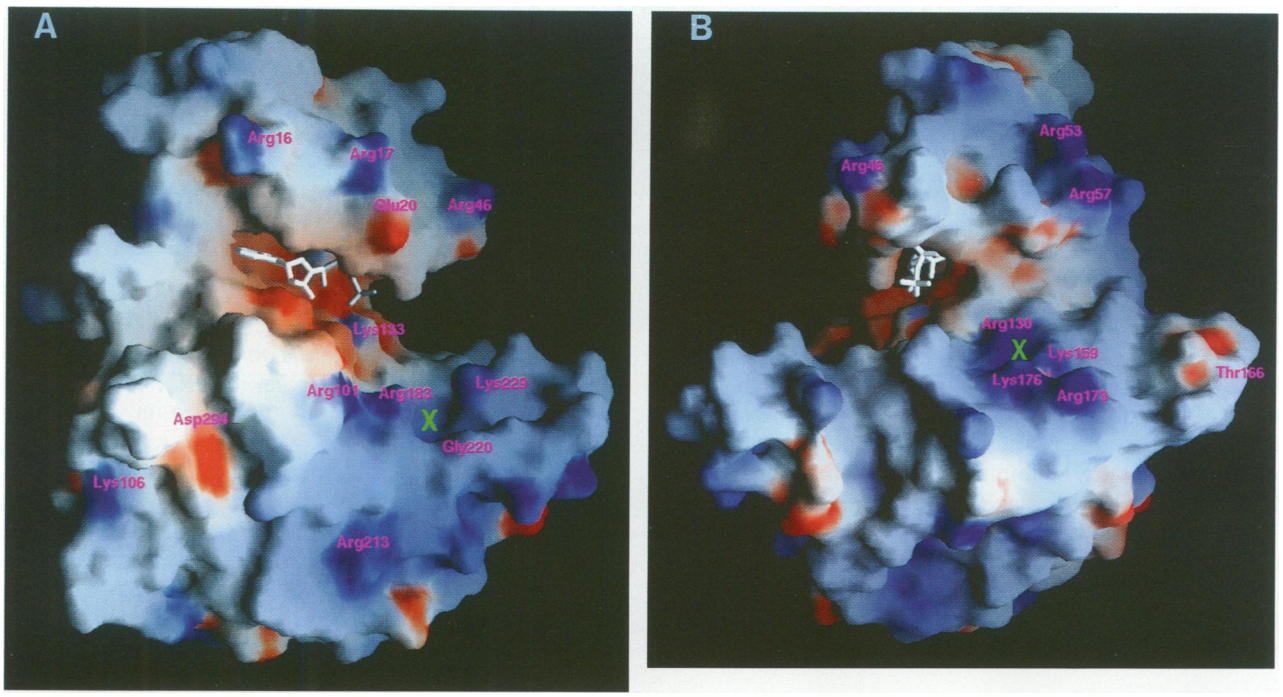

Fig. 4. Molecular surface of CK1. The surface charge distribution of Cki1Δ298 was computed at neutral pH using the program GRASP (Nicholls *et al.*, 1991) and displayed at the level of the solvent-accessible surface, assuming the probe radius of 1.4 Å to represent a water molecule, and the dielectric constants of 80 and 2 for the solvent and protein, respectively. Color-coded blue for positive (20 k_BT), red for negative (−20 k_BT), and white for neutral, where k_B is the Boltzmann's constant and T is the temperature. The MgATP is in stick model. (**A**) The location of the sulfate-binding site S1 is indicated by a green cross. The S1 site lies in the cleft where it may bind the phosphate moiety of phosphoprotein substrates. (**B**) The location of the sulfate-binding site S2 is indicated by a green cross. The S2 site marks a possible autophosphorylation site in CK1.

respectively. Despite these differences, the peptide substrate bound with cAPK (Knighton *et al.*, 1991b) could still be modelled in a similar location on the surface of the alpha lobe of CK1. As mentioned above, all known forms of CK1 are positively charged at neutral pH. The positive charges are enriched in the substrate-binding region (Figure 4), where they are in positions to make contact with the acidic residues N-terminal to the phosphorylatable hydroxyamino acid of peptide substrate.

A sulfate anion (the S1 site) has been identified in the positively charged peptide substrate-binding region (Figure 4A), where it may mimic the non-covalent binding of a phosphate ion or phosphohydroxyamino acid as it does in the structures of other phosphoproteins (Barford and Johnson, 1989; Volz and Matsumura, 1991). The S1 site is comprised of the main chain nitrogen of Gly220, the ε-amino nitrogen of Lys229, and the guanidino moiety of Arg183 (Figure 5A). Each of these residues is conserved throughout the CK1 family. Arg183, which is found in all CK1 isoforms except mammalian CKIβ (Rowles *et al.*, 1991), occupies the same positions as does Glu203 in cAPK. This residue (Glu203 in cAPK) contacts P^{-3} and P^{-6} of PKI (Knighton *et al.*, 1991b), and in part defines the substrate selectivity of cAPK. Thus, the S1 binding site

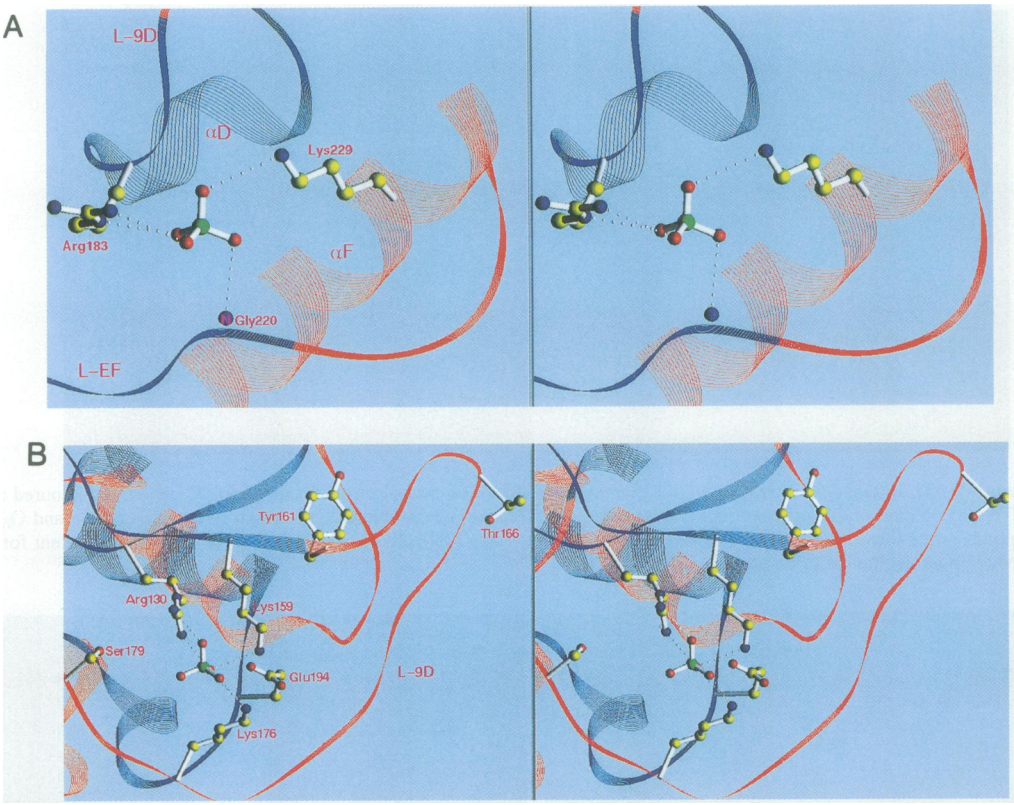

Fig. 5. (**A**) The structural basis of substrate selectivity of CK1. The side chains of Arg183 from L-9D and Lys229 from αF and the main chain nitrogen of Gly220 from L-EF form the sulfate-binding site S1. (**B**) Sulfate-binding site S2 resembles an autophosphorylation site in cAPK. The S2 site formed by the side chains of Arg130, Lys159, and Lys176. Lys159 and Lys176 also interact with Glu194.

may explain why CK1 binds synthetic peptide substrates containing phosphoamino acids in the P^{-3} position with greater affinity than identical peptides containing simple acidic residue in this position. The S1 site also suggests a mechanism for CK1 inhibition by phosphatidylinositol-4,5-bisphosphate (Brockman and Anderson, 1991). Gly220 in CK1 is followed by a three-residue insertion unique to the CK1 family that is part of five disordered residues (Lys222−Asn226) in loop L-EF. If this loop normally interacts with peptide substrate, then its flexibility may result from the absence of peptide substrate in the crystal.

Phosphorylation sites

We have shown that the CK1 isoforms are highly phosphorylated *in vivo* (Hoekstra *et al.*, 1994), and that the catalytic domain of Cki1 can contain at least 1.5 mol/mol phosphate (Carmel *et al.*, 1994). Although our structure is of unphosphorylated CK1, the identification of a second sulfate anion (the S2 site) reveals the possible location of a phosphate moiety present in phospho-CK1 (Figure 4B). The sulfate is in contact with three positively charged side chains, Arg130, Lys159 and Lys176, each of which is conserved among CK1 family (Lys or Arg is found in position 130 in all isoforms except mammalian CKIβ and Hhp2) (Figure 5B). When the structures of CK1 and cAPK are superimposed, the sulfate lies within 1.2 Å of the phosphate group of phospho-Thr197 in cAPK. Moreover, Arg130 and Lys159 of CK1 occupy the same positions as Arg165 and Lys189 in cAPK, which chelate phospho-Thr197. Thus, the S2 site may mark the position of an autophosphorylation site analogous to Thr197 in cAPK. The side chain closest to the sulfate capable of being phosphorylated is Ser179 in CK1. Serine in this position can be replaced by threonine in some other isoforms.

Potential regulatory mechanisms

Alternative phosphorylation sites are apparent from inspection of loop L-9D (Tyr161−Met185), the homolog of the 'activation loop' identified in other protein kinases between the conserved DFG and APE sequence motifs where phosphorylation sites are commonly found in other protein kinases (Morgan and De Bondt, 1994; Taylor and Radzio-Andzelm, 1994). The homologous loop in Cdk2 (the T-loop) contains at its apex the regulatory phosphorylation site, Thr160, that must be phosphorylated for full Cdk2 activity. The possible homolog in CK1 is invariant Thr166 (and/or Tyr161) in the beginning of loop L-9D, where it may mediate CK1 regulation by reversible phosphorylation. Thr166 is exposed on the surface, and is therefore likely to be accessible. Tyr161 is buried and its indole ring lies nearly parallel to the hydrophobic part of the side chains of Arg162 and Arg197 on either side.

Discussion

Regardless of its source, CK1 purifies as a constitutively active monomer with full protein kinase activity (Tuazon and Traugh, 1991), and phosphorylation is not required for proper folding of Cki1Δ298 in bacteria or for expression of its full catalytic activity (Carmel *et al.*, 1994). Yet the importance of CK1 for cell function suggests that its

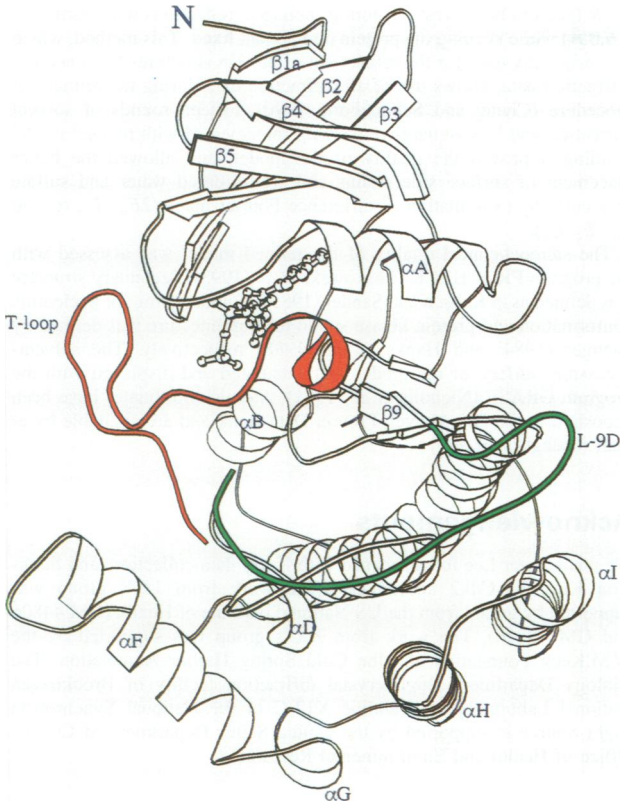

Fig. 6. The 'activation loop' in CK1. The loop L-9D (green) in CK1 is rotated ~180° with respect to T-loop (red) in Cdk2 and the two loops lie opposite each other. Thus, the peptide-binding region in CK1 is fully accessible to substrate.

various isoforms are under some form of regulation (Dhillon and Hoekstra, 1994; Wang *et al.*, 1994). The structure of loop L-9D suggests it plays a role in the regulation of CK1. Initially, L-9D contains Lys159 and Lys176 which interacts with a sulfate (the S2 site) in our dephospho-structure of CK1 but, as described above, may bind a phosphate moiety in phospho-CK1. Secondly, the loop L-9D is longer than comparable loops in cAPK and Cdk2 and contains three possible phosphorylatable amino acids, Tyr161, Thr166 and Ser179. Thirdly, in the structure of inactive Cdk2, the T-loop rises from the alpha lobe to make contact with the glycine-rich flap, and is positioned to control Cdk2 activity by reversibly blocking its active site (De Bondt *et al.*, 1993). In our model of unphosphorylated, fully active CK1, the loop L-9D is in an open conformation, leaving the active site accessible to substrate (Figure 6). The two conformations may be interchangeable. It has been suggested that upon Cdk2 activation, the small helix N-terminal to the T-loop (αL12) unwinds, removing the T-loop from the active site (De Bondt *et al.*, 1993), whence it may adopt a conformation similar to that of L-9D in CK1. Similarly, an *in vivo* regulatory mechanism may stabilize L-9D in a conformation similar to that observed for the T-loop in inactive Cdk2. The capability of L-9D being phosphorylated suggests that CK1 may be a substrate for the cdk-activating kinase MO15 (Soloman *et al.*, 1993) or related enzymes. The phosphorylation of Thr166 in CK1 may be responsible for the cell cycle-dependent localization of mammalian CK1 (Brockman *et al.*, 1992), and for regulation of cytoplasmic yeast CK1, which has been implicated in the switch between apical and isotropic bud growth (Vancura *et al.*, 1994). The conservation of Tyr161 in the CK1 family, its location in the regulatory loop L-9D, and its capability of being phosphorylated suggest the function of this residue in the CK1 regulation. The buried status of Tyr161 observed in this structure also suggests that the phosphorylation of Tyr161 may cause local conformational change.

Evidence that CK1 activity is directly regulated by mechanisms other than association with phosphatidylinositol-4,5-bisphosphate has been elusive (Issinger, 1993). Thus, CK1 and Cdk2 may be regulated in different ways, although they share similarities in structure. Our model points to a second potential mechanism for CK1 regulation: L-9D may regulate the reversible association of CK1 with the cytoskeletal fraction. Included in L-9D is a sequence motif, His169-Ile-Pro-Tyr-Arg-Glu-Lys175, found in the head regions of kinesins, the motor proteins of microtubules (Roof *et al.*, 1992). The head region contains microtubule-binding sequences, of which the motif may be a component (Goldstein, 1991). Isoforms of CK1 copurify with cytoskeletal proteins (Floyd *et al.*, 1991), and may associate with them in part through the motif.

One Mg^{2+} was identified on the basis of its bonding distances and coordination geometry as a homolog of the low-affinity M1 site of cAPK (Bossemeyer *et al.*, 1993; Zheng *et al.*, 1993). Although cAPK contains a second Mg^{2+} bridging the β- and γ-phosphates (the M2 site), no density for this site was observed in CK1. In cAPK, reduced phosphotransferase velocity accompanies occupation of the low-affinity M1 site (Cook *et al.*, 1982). Our results suggest that the primary role of Mg^{2+} is to provide an electron sink for the γ-phosphorus by directly binding in either the M2 or M1 position. As demonstrated through kinetic measurements, the binding of a second Mg^{2+} increases the affinity of ATP for kinase by decreasing its dissociation rate (Kong and Cook, 1988). Because the dissociation rate of ADP product is also reduced, and because this is the rate-limiting step, the overall rate of phosphoryltransfer is diminished. Thus, the occupation of both M1 and M2 sites by Mg^{2+} appears to be inhibitory. Our finding in CK1 suggests that protein kinase activity requires binding of one Mg^{2+} rather than occupation of a specific site, and that binding of additional ion(s) to either site leads to inhibition through decreased product dissociation. Thus, the location of the highest-affinity Mg^{2+}-binding site may vary among protein kinases.

An intriguing feature of CK1 is the triplet Ser186-Ile-Asn188 of helix αD that replaces the triplet Ala-Pro-Glu found in cAPK, Cdk2 and most other protein kinases. In both cAPK and Cdk2, the glutamic acid of the triplet forms an ion pair with an arginine that is located in a loop homologous to L-HI in CK1 (De Bondt *et al.*, 1993; Zheng *et al.*, 1993). Surprisingly, the Ser-Ile-Asn motif adopts the same secondary structure and is in the same location as the Ala-Pro-Glu sequence of cAPK. Instead of ion-pairing formation, however, Ser186 and Asn188 hydrogen bond to Arg198 and Asp199 of helix αE respectively, whereas the side chain of Ile187 is buried. A novel ion pair between Glu202 of αE and Arg261 of αH confers additional stability.

In summary, CK1 is a conserved member of the eukaryotic protein kinase family despite its unusual

primary structure. Its most divergent motifs appear to shape its unique substrate specificity and participate in its regulation. The genetically tractable CK1 homologs of fission yeast will prove useful in testing these hypotheses, and in correlating structure with *in vivo* function.

Materials and methods

Crystallization

Cki1Δ298 was overexpressed, purified, and crystallized as described by Carmel *et al.* (1994). The crystals were grown by mixing the protein (0.3 mM in 10 mM MOPS pH 7.0, 0.1 mM EDTA, 0.1% 2-mercaptoethanol, 1 mM dithiothreitol and 200 mM NaCl) in the presence of 6 mM ATP/1.5 mM MgCl with mother liquor (1.55 mM ammonium sulfate, 50 mM sodium citrate, pH 5.6) and equilibrating the mixture against 1 ml of the latter solution at 16°C. The crystal formed in trigonal space group $P3_221$ with one complex (one molecule of Cki1Δ298 and one MgATP) in each of the six asymmetric units and ~55% of solvent content.

Data collection

Trigonal crystals were subjected to X-ray diffraction on a FAST television area detector (Enraf–Nonius) at beamline X12-C of the National Synchrotron Light Source (Brookhaven National Laboratory). Data collection parameters were as follows: the wavelength was 1.0 Å for native crystals, the exposure times were 5 or 10 s every 0.1° rotation at 2.5 GeV, ≈200–110 mA, and the detector was run at a gain setting of SETDET 7 1 or 5 1. Anomalous differences were determined from Bijvoet pairs that were measured simultaneously by aligning the crystals with the *c*-axis parallel to the rotation axis.

Two mercurial derivatives were prepared by adding either *p*-chloromercuribenzene sulfonate (*p*CMBS) or 1,4-diacetoxymercuri-2,3-dimethoxybutane (Baker's dimercurial) directly to hanging droplets at 1 mM final concentration and incubating the resultant mixture for 24 h at 16°C. Derivatization of the crystals was monitored prior to data collection by assaying the Hg L_{III} absorption edge (12.286 keV) through X-ray fluorescence measurements. When collecting derivative datasets, the incident energy was adjusted to 90 eV above the Hg L_{III} absorption edge to enhance anomalous signals (i.e. λ = 1.0012 Å).

Phasing

Heavy atom refinement, solvent leveling, phase combination, phase and map calculation, and skeleton generation were performed with the program package PHASES (Furey and Swaminathan, 1990) on the data sets summarized in Table I. The first heavy-atom position was identified from difference and anomalous scattering Patterson maps (both mercurial compounds bound Cys99 with full occupancy). The initial 3.0 Å multiple isomorphous replacement with anomalous scattering (MIRAS) phases were improved by four, four and eight cycles of solvent leveling (Wang, 1985) following each of three envelope determinations using a solvent content of 30%. A skeleton representation of the resultant electron density map was generated, and a partial poly-alanine chain was built for ~60% of the structure. This partial model was used to improve the phases by phase combination with the solvent-flattened MIRAS phases. The resultant phases, which were further improved by density histogram matching and constraint of local density shape using the program SQUASH (Zhang, 1993), allowed identification of a second heavy-atom site (both derivatives bound Cys246 with <35% occupancy). Using two sites for each derivative, a new multiple isomorphous replacement (MIR) map was calculated.

Model building and refinement

A starting Cα backbone trace was built into the 3.0 Å MIR map using the graphics program 'O' (Jones *et al.*, 1991). Five rounds of phase combination using a poly-alanine model and MIR phases enabled us to recognize most of the side chains of the known amino acid sequence (Wang *et al.*, 1994), and to identify one ATP molecule. The resultant model was refined by simulated annealing and least-squares minimization using the program suite X-PLOR (Brünger *et al.*, 1989). For refinement, the diffraction data were extended to include all measured reflections (11.3–2.0 Å resolution), and were subjected to bulk solvent correction using X-PLOR. The unit cells of the crystals were divided into protein and solvent components. Two parameters that describe the solvent component, a solvent scattering density and an isotropic temperature factor, were determined by an iterative search for the value that minimizes the *R*-factor in the lowest resolution shell (875 reflections with resolution <6.0 Å) while keeping the protein component fixed. This method, which was originally used for the refinement of protein structures from neutron diffraction data, allows use of all diffraction data during the refinement procedure (Cheng and Schoenborn, 1990). Fifteen rounds of solvent correction and least-squares refinement interspersed with manual model building improved the quality of the model, and allowed the better placement of surface side chains and well-ordered water and sulfate molecules by examination of difference Fourier maps ($2F_o-F_c$, α_c and F_o-F_c, α_c).

The stereochemical quality of the refined model was assessed with the program PROCHECK (Laskowski *et al.*, 1993). Secondary structure was defined as in Kabsch and Sander (1983). Nomenclature for nucleotide conformation and protein kinase subdomain architecture was defined by Saenger (1984) and Hanks *et al.* (1988) respectively. The solvent-accessible surface of the model was calculated and displayed with the program GRASP (Nicholls *et al.*, 1991). Atomic coordinates have been deposited in the Brookhaven Protein Data Bank and are available by e-mail (cheng@cshL.org).

Acknowledgements

We thank Peter Lee for assistance with X-ray data collection, and Sung-Hou Kim for Cdk2 coordinates. The work from J.K's group was supported by grants from the US National Institute of Health (GM 44806 and GM 48216). The work from X.C's group was supported by the W.M.Keck Foundation and the Cold Spring Harbor Association. The Biology Department single-crystal diffraction facility of Brookhaven National Laboratory at beamline X12-C of the National Synchrotron Light Source is supported by the United States Department of Energy, Office of Health and Environmental Research.

References

Barford,D. and Johnson,L.N. (1989) *Nature*, **340**, 609–619.
Bossemeyer,D., Engh,R.A., Kinzel,V., Ponstingl,H. and Huber,R. (1993) *EMBO J.*, **12**, 849–859.
Brockman,J.L. and Anderson,R.A. (1991) *J. Biol. Chem.*, **266**, 2508–2512.
Brockman,J.L., Gross,S.D., Sussman,M.R. and Anderson,R.A. (1992) *Proc. Natl Acad. Sci. USA*, **89**, 9454–9458.
Brünger,A.T., Karplus,M. and Petsko,G.A. (1989) *Acta Crystallogr.*, **A45**, 50–61.
Carmel,G., Leichus,B. Cheng,X., Patterson,S.D., Mirza,U., Chait,B.T. and Kuret,J. (1994) *J. Biol. Chem.*, **269**, 7304–7309.
Cegielska,A. and Virshup,D.M. (1993) *Mol. Cell Biol.*, **13**, 1202–1211.
Cheng,X. and Schoenborn,B.P. (1990) *Acta Crystallogr.*, **B46**, 195–208.
Chijwa,T., Hagiwara,M. and Hidaka,H. (1989) *J. Biol. Chem.*, **264**, 4924–4927.
Cook,P.F., Neville,M.E., Vrana,K.E., Hartl,F.T. and Roskoski,J.R. (1982) *Biochemistry*, **21**, 5794–5799.
De Bondt,H.L., Rosenblatt,J., Jancarik,J., Jones,H.D., Morgan,D.O. and Kim,S.-H. (1993) *Nature*, **363**, 595–602.
De Groot,R.P., den Hertog,J., Vandenheede,J.R., Goris,J. and Sassone-Corsi,P. (1993) *EMBO J.*, **12**, 3903–3911.
Dhillon,N. and Hoekstra,M.F. (1994) *EMBO J.*, **13**, 2777–2788.
Flotow,H., and Roach,P.J. (1991) *J. Biol. Chem.*, **266**, 3724–3727.
Flotow,H., Graves,P.R., Wang,A., Fiol,C.J., Roeske,R.W. and Roach,P.J. (1990) *J. Biol. Chem.*, **265**, 14264–14269.
Floyd,C.C., Grant,P., Gallant,P.E. and Pant,H.C. (1991) *J. Biol. Chem.*, **266**, 4987–4994.
Furey,W. and Swaminathan,S. (1990) *American Crystallographic Association Meeting Abstracts*, Series 2, Vol. 18, p. 73.
Goldstein,L.S.B. (1991) *Trends Cell Biol.*, **1**, 93–98.
Hanks,S.K., Quinn,A.M. and Hunter,T. (1988) *Science*, **241**, 42–52.
Hoekstra,M.F., Liskay,R.M., Ou,A.C., DeMaggio,A.J., Burbee,D.G. and Heffron,F. (1991) *Science*, **253**, 1031–1034.
Hoekstra,M.F., Dhillon,N., Carmel,G., DeMaggio,A.J., Lindberg,R.A., Hunter,T. and Kuret,J. (1995) *Mol. Cell. Biol.*, **15**, in press.
Issinger,O.-G. (1993) *Pharmacol. Ther.*, **59**, 1–30.
Jones,T.A., Zou,J.Y., Cowan,S.W. and Kjeldgaard,M. (1991) *Acta Crystallogr.*, **A47**, 110–119.
Kabsch,W. and Sander,C. (1983) *Biopolymers*, **22**, 2577–2637.
Karlsson,R., Zheng,J., Xuong,N.-H., Taylor,S.S. and Sowadski,J.M. (1993) *Acta Crystallogr.*, **D49**, 381–388.

Kearney,P., Ebert,M. and Kuret,J. (1994) *Biochim. Biophys. Res. Commun.*, **203**, 231–236.
Knighton,D.R., Zheng,J., Ten Eyck,L.F., Ashford,V.A., Xuong,N.-H., Taylor,S.S. and Sowadski,J.M. (1991a) *Science*, **253**, 407–414.
Knighton,D.R., Zheng,J., Ten Eyck,L.F., Ashford,V.A., Xuong,N.-H., Taylor,S.S., and Sowadski.J.M. (1991b) *Science*, **253**, 415–420.
Kong,C.-T. and Cook,P.F. (1988) *Biochemistry*, **27**, 4795–4799.
Kuret,J., Woodgett,J.R. and Cohen,P. (1985) *Eur. J. Biochem.*, **151**, 39–48.
Laskowski,R.A., MacArthur,M.W., Moss,D.S. and Thornton,J.M. (1993) *J. Appl. Crystallogr.*, **26**, 283–291.
Meggio,F., Perich,J.W., Reynolds,E.C. and Pinna,L.A. (1991) *FEBS Lett.*, **283**, 303–306.
Milne,D.M., Palmer,R.H., Campbell,D.G. and Meek,D.W. (1992) *Oncogene*, **7**, 1361–1369.
Morgan,D.O. and De Bondt,H.L. (1994) *Curr. Opin. Cell Biol.*, **6**, 239–246.
Nicholls,A., Sharp,K.A. and Honig,B. (1991) *Proteins: Struct. Funct. Genet.*, **11**, 281–296.
Ramachandran,G.N., Ramakrishnan,C. and Sasiekharan,V. (1963) *J. Mol. Biol.*, **7**, 95–99.
Roach,P.J. (1991) *FASEB J.*, **4**, 2961–2968.
Robinson,L.C. *et al.* (1992) *Proc. Natl Acad. Sci. USA*, **89**, 28–32.
Roof,D.M., Meluh,P.B. and Rose,M.D. (1992) *J. Cell Biol.*, **118**, 95–108.
Rowles,J., Slaughter,C., Moomaw,C., Hsu,J. and Cobb,M.H. (1991) *Proc. Natl Acad. Sci USA*, **88**, 954–955.
Saenger,W. (1984) *Principles of Nucleic Acid Structure*. Springer-Verlag, New York.
Soloman,M.J., Harper,J.W. and Shuttleworth,J. (1993) *EMBO J.*, **12**, 3133–3142.
Taylor,S.S. and Radzio-Andzelm,E. (1994) *Structure*, **2**, 345–355.
Tuazon,P.T. and Traugh,J.A. (1991) *Adv. Sec. Mess. Phosphoprot. Res.*, **23**, 123–164.
Umpress,J.L., Tuazon,P.T., Chen,C.-J. and Traugh,J.A. (1992) *Eur. J. Biochem.*, **203**, 239–243.
Vancura,A., Sesler,A., Leichus,B. and Kuret,J. (1994) *J. Biol. Chem.*, **269**, 19271–19278.
Vincent,I.J. and Davies,P. (1993) *Proc. Natl Acad. Sci. USA*, **89**, 2878–2882.
Volz,K. and Matsumura,P. (1991) *J. Biol. Chem.*, **266**, 15511–15519.
Wang,B.C. (1985) *Methods Enzymol.*, **115**, 90–112.
Wang,P.C., Vancura,A., Mitcheson,T. and Kuret,J. (1992) *Mol. Cell. Biol.*, **3**, 275–286.
Wang,P.C., Vancura,A., Desai,A., Carmel,G. and Kuret,J. (1994) *J. Biol. Chem.*, **269**, 12014–12023.
Zhang,K.Y.J. (1993) *Acta Crystallogr.*, **A49**, 213–222.
Zheng,J., Knighton,D.R., Ten Eyck,L.F., Karlsson,R., Xuong,N.-H., Taylor,S.S. and Sowadski,J.M. (1993) *Biochemistry*, **32**, 2154–2161.

Received on October 25, 1994; revised on December 8, 1994